

Contrast enhancement pattern on multidetector CT predicts malignancy in pancreatic endocrine tumours

Carla Cappelli · Ugo Boggi · Salvatore Mazzeo · Rosa Cervelli · Daniela Campani · Niccola Funel · Benedetta Pontillo Contillo · Carlo Bartolozzi

Received: 14 March 2014 / Revised: 11 September 2014 / Accepted: 3 November 2014 / Published online: 2 December 2014
© European Society of Radiology 2014

Abstract

Objectives Preoperative suspicion of malignancy in pancreatic neuroendocrine tumours (pNETs) is mostly based on tumour size. We retrospectively reviewed the contrast enhancement pattern (CEP) of a series of pNETs on multiphasic multidetector computed tomography (MDCT), to identify further imaging features predictive of lesion aggressiveness.

Methods Sixty pNETs, diagnosed in 52 patients, were classified based on CEP as: type A showing early contrast enhancement and rapid wash-out; type B presenting even (B1) or only (B2) late enhancement. All tumours were resected allowing pathologic correlations.

Results Nineteen pNETs showed type A CEP (5–20 mm), 29 type B1 CEP (5–80 mm) and 12 type B2 (15–100 mm). All tumours were classified as well differentiated tumours, 19 were benign (WDt-b), 15 with uncertain behaviour (WDt-u) and 26 carcinomas (WDC). None of A lesions were malignant (12 WDt-b; 7 WDt-u), all B2 lesions were WDC, 7 B1 lesions were WDt-b, 8 WDt-u and 14 WDC; 4/34 (12 %) lesions ≤ 2 cm were WDC.

CEP showed correlation with all histological prognostic indicators.

Conclusions Correlating with the lesion grading and other histological prognostic predictors, CEP may preoperatively suggest the behaviour of pNETs, assisting decisions about treatment. Moreover CEP allows recognition of malignant small tumours, incorrectly classified on the basis of their dimension.

Key Points

- Neuroendocrine pancreatic tumours (pNETs) show different post-contrast behaviour on CT.
- pNETs can be classified on the basis of contrast enhancement into three categories.
- CT classification of pNETs shows strong correlation with histological prognostic factors.
- CT pattern may suggest the optimal management of pNETs.

Keywords Pancreas · Neuroendocrine tumours · Multidetector computed tomography · Prognosis · Neoplasm grading

C. Cappelli · S. Mazzeo · R. Cervelli · B. P. Contillo · C. Bartolozzi
Diagnostic and Interventional Radiology, Department of Translational Research and New Technologies in Medicine and Surgery, University of Pisa, Pisa, Italy

U. Boggi
General and Transplant Surgery, Department of Translational Research and New Technologies in Medicine and Surgery, University of Pisa, Pisa, Italy

D. Campani · N. Funel
Pathology, Department of Surgical, Medical, Molecular and Critical Area Pathology, University of Pisa, Pisa, Italy

C. Cappelli (✉)
Azienda Ospedaliero-Universitaria Pisana-Radiodiagnostica I, Via Paradisa 2, 56124 Pisa, Italy
e-mail: carlacappelli1@gmail.com

Introduction

Pancreatic endocrine tumours (pNETs) represent 1–3 % of pancreatic neoplasms, with an annual incidence of 1–1.5 per 100,000 persons per year [1–4]. These tumours may occur in inherited syndromes [von-Hippel-Lindau (VHL) disease; multiple endocrine neoplasia type 1 (MEN-1); neurofibromatosis type 1; tuberous sclerosis], but are usually sporadic.

Although rare, these diseases have different prognosis and therapeutic management (both medical and surgical) compared to others pancreatic neoplasms, and therefore require correct identification. Moreover, pNETs include a heterogeneous group of tumours that show a wide range of morphological, functional and behavioural characteristics, reflected in a

large spectrum of clinical presentation, with significant differences in survival rates [1–6] and reflected in the lack of uniform pathological classifications and staging systems [1, 2, 5, 7–10]. For these reasons, the need to stratify patients into risk categories for correct therapeutic management has led to the identification of postoperative prognostic factors [5, 11–13]. In recent years, the guidelines developed by the European Neuroendocrine Tumor Society (ENETS) and the 2010 revised version of the World Health Organization (WHO) underlined the concept that all pNETs have a malignant potential and proposed a new grading system based on the Ki67 proliferative index, which proved to be an effective and independent predictor of survival in several studies [3, 14–17].

However, the biologic course of pNETs can be accurately predicted on the basis of pathology parameters [5, 11–13] which, unfortunately, cannot be fully assessed until the entire tumour has been resected [8]. On the contrary, when obvious landmarks of malignancy are lacking, tumour size is the only reliable preoperative parameter used to discriminate between presumably benign, uncertain and malignant pNETs, it being generally accepted that pNETs exceeding 2 cm in their largest diameter may have borderline pathology or even harbour malignancy [8].

Imaging of the lesion location and spreading is mandatory to determine whether surgical resection for possible cure or debulking is needed or to determine whether medical treatment for advanced metastatic disease is appropriate. However, only few studies have been focused on additional imaging characteristics useful for the assessment of pNET aggressiveness [18–20]. Among these, two studies published in 2005 and 2009 [19, 20] demonstrated that the microvascular density (MVD) and the vascular endothelial growth factor (VEGF) expression correlate with the lesion grade (the MVD being significantly lower in malignant lesions) and that some perfusion CT parameters are strongly correlated with the MVD and with a number of other prognostic indicators of lesion nature.

In this study we retrospectively reviewed a contemporary series of pNETs undergoing standardized preoperative evaluation by means of multiphasic contrast-enhanced multidetector computed tomography (MDCT), with the aim of evaluating the capability of characterizing the biological aggressiveness of pNETs on the basis of their post-contrast behaviour.

Methods

Patient population

Between July 2005 and September 2013, 60 pNETs were resected in 52 consecutive patients (21 men, 31 women; mean age 57 years, range 24–82 years). Four patients were diagnosed with MEN-1 syndrome.

MDCT study protocol

All patients underwent preoperative MDCT using either a 4- or a 64-row scanner (Light Speed Plus, GE Medical System, Milwaukee, USA; Light Speed Plus VCT, GE Medical System, Milwaukee USA) according to a standardized evaluation protocol.

Following precontrast imaging, high-concentration iodinated contrast medium (iomeprol 81.65 g/100 mL, 400 mg iodine/mL) was injected intravenously at a flow rate of 4–5 mL/s, using a dual-head pump injector. Post-contrast CT imaging included four phases: early arterial phase (at 15–20 s), pancreatic phase (at 35–40 s), venous phase (at 70 s) and late phase (at 180 s). The imaging parameters were slice thickness, 2.5–1.25 mm; reconstruction interval, 1.25–0.625 mm; beam pitch, 1.5 or 0.984:1; tube voltage, 100–120 kV; 300–350 mA or automatic tube current modulation (smart mA, noise index 21); 0.6/0.8-s rotation speed; 512 matrix size.

Imaging data analysis

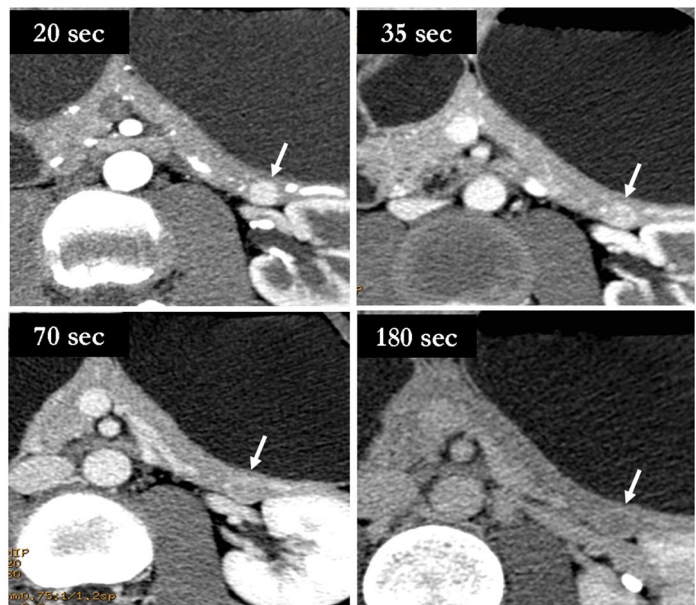
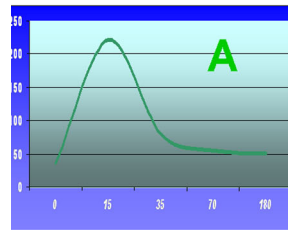
A qualitative analysis of the contrast enhancement pattern (CEP) in different subsequent phases was performed and two main CEPs of pNETs were defined. Tumours showing early contrast enhancement (during arterial or pancreatic phase) and rapid wash-out, resulting in isodense appearance relative to the parenchyma in the venous/late phases, were classified as type A CEP (Fig. 1). Tumours showing contrast enhancement in venous and late phases were classified as type B CEP; among these lesions, tumours having also early contrast enhancement were subclassified as B1 (Fig. 2), while those showing delayed contrast enhancement alone were classified as type B2 (Fig. 3).

The largest tumour diameter was also measured.

Histological analysis

Tissue slices (1–5 μ m) from paraffin-embedded blocks were cut and stained with haematoxylin–eosin. Tumours were classified as endocrine on the basis of the histological examination of the haematoxylin–eosin staining and of immunohistochemical expression of both chromogranin (clone DAK-A3; Dako, Carpinteria, CA, USA) and synaptophysin (clone SY38; Dako, Milan, Italy). For each tumour, features recorded were tumour differentiation (according to both the WHO 2004 criteria and the ENETS 2006 criteria); tumour size; presence of angioinvasion and perineural invasion; presence of regional lymph node and distant metastases; mitotic rate and Ki67 labelling index by MIB-1 antibody (DAKO, Milano, Italy); tumour stage [according both to the American Joint Committee on Cancer and International Union Against

Fig. 1 CT appearance of a lesion presenting A CEP: the small nodular lesion of the pancreatic tail (*arrows*) shows an early enhancement, during early arterial (20 s) and pancreatic (35 s) phases, with wash-out in venous (70 s) and late (180 s) phases. The graph on the left side is representative of the enhancement trend



Cancer (AJCC–UICC) 2009 and the ENETS 2006 staging systems].

Quantification of microvascular density (MVD) was performed by CD34 immunostaining (QBEND10, Immunotech, Marseille, France), by vessel count per field (6 hypervascular fields per case, at a magnification of $\times 20$, yielding a surface area of 0.588 mm^2 for each field). The total area analysed for each sample was 3.528 mm^2 .

The presence of fibrosis was evaluated in all specimens and graded as follows: class I, having a percentage of fibrosis of less than 25 % of the microscopic field ($\times 10$, in haematoxylin–eosin stained slides); class II, fibrosis between 25 and 50 %; class III, with fibrosis greater than 50 % (Fig. 4).

Statistical analysis

Data obtained from MDCT examination (CEP of each tumour) were compared to those obtained at histology after surgical resection, including maximum lesion diameter; histological type; Ki67 value; presence of angioinvasion, nodal and distant metastases; stage of the lesion (according both to the AJCC–UICC system and the ENETS stage system); MVD.

Descriptive statistics (proportions, means, standard deviation) were calculated for patient characteristics and numeric continuous data. The χ^2 , Pearson and Fisher exact tests were used for categorical data, whereas continuous data were

Fig. 2 CT post-contrast appearance of a lesion presenting B1 CEP: the lesion of the pancreatic head (*arrows*) shows wash-in early arterial (20 s) and pancreatic (35 s) phases, with persistence of the enhancement in venous (70 s) and late (180 s) phases. The graph on the left side is representative of the enhancement trend

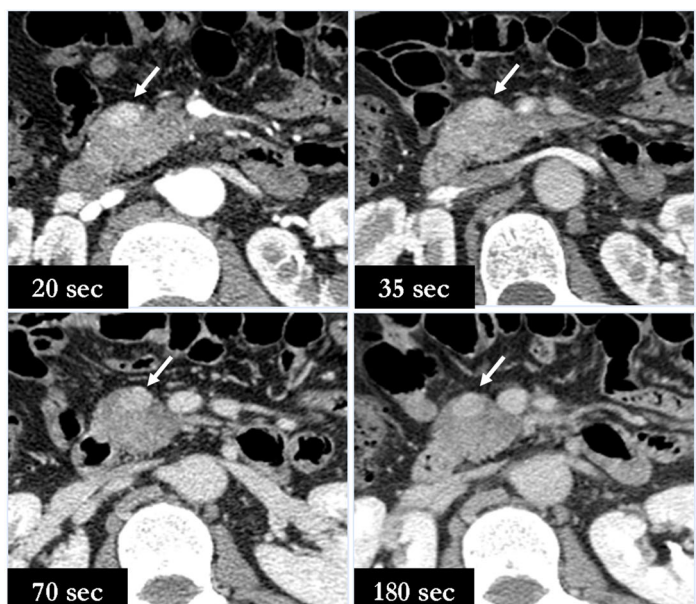
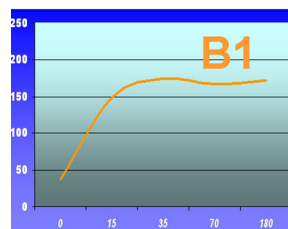
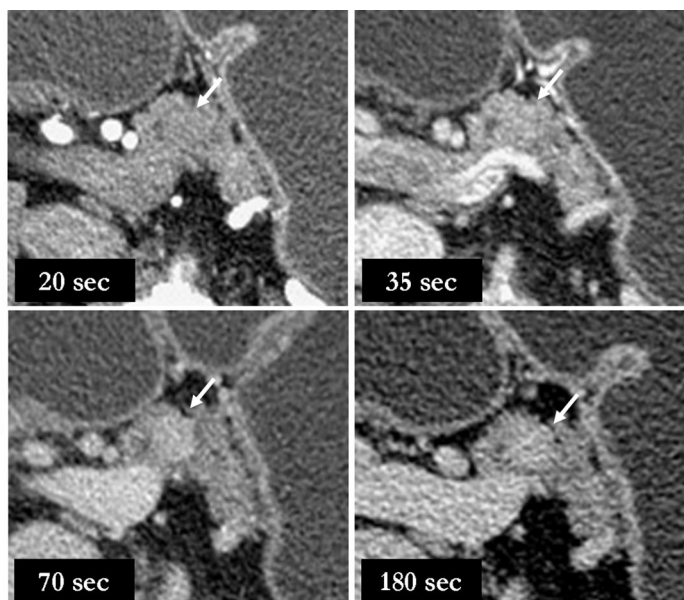
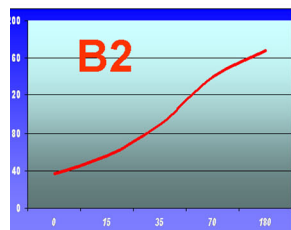


Fig. 3 CT post-contrast appearance of a B2 lesion: the nodule of the pancreatic body (arrows) shows enhancement only in venous (70 s) and late (180 s) phases. The graph on the left side is representative of the enhancement trend



evaluated by bivariate fit, one-way analysis of variance and Student *t* test.

A *p* value of 0.05 or less was considered to indicate significance.

Results

MDCT pattern

MDCT identified 60 pNETs in 52 patients. Forty-eight patients had one pNET each, while 4 patients had multiple pNETs. One patient had two synchronous sporadic pNETs, while the remaining 3 patients had 2, 3 and 5 pNETs, respectively, occurring in the setting of MEN-1 syndrome. Liver metastases were identified in 11 patients (21 %) and infiltration of main peripancreatic veins was suspected in 8 patients (15 %) (3 SMV, 5 splenic vein), indicating malignant tumour histology.

The largest diameter of tumours was less than 2 cm in 28 lesions and at least 2 cm in the remaining 32 lesions.

Type A CEP (Table 1) was identified in 19 pNETs (32 %), with the diameter ranging between 5 and 20 mm [average diameter at CT (adCT) 11 mm]. Type B CEP was identified in 41 pNETs (5–100 mm; adCT 35 mm); of these, 29 (48 %) lesions showed type B1 CEP (5–80 mm; adCT 31 mm), and 12 (20 %) showed type B2 CEP (15–100 mm; adCT 44 mm).

Resection of pNETs

Primary pNETs were resected in all patients allowing full comparison between radiologic and pathologic parameters. Surgery was carried out by robot-assisted laparoscopy in 4 patients and by conventional surgery in the remaining 48 patients. Four patients underwent tumour enucleation, 23 distal pancreatectomy with ($n=15$) or without ($n=8$) splenectomy, 21 pancreaticoduodenectomy, 3 central pancreatectomy and 1 total pancreatectomy. Mesenteric/portal vein resection

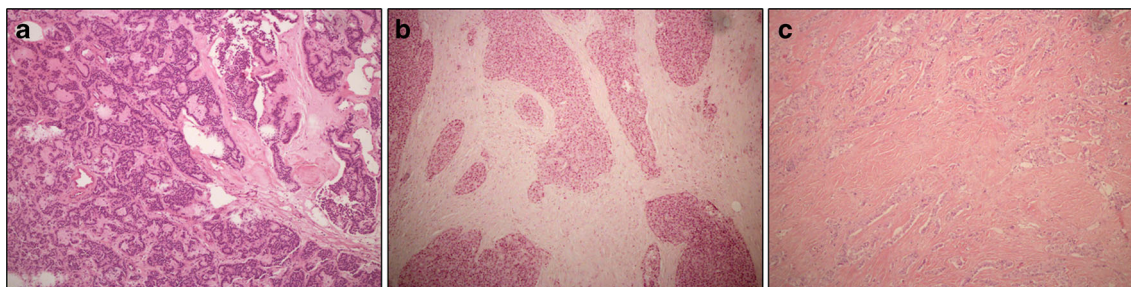


Fig. 4 Fibrosis rating in pNETs, expressed as a percentage of the microscopic field ($\times 10$, in haematoxylin–eosin stained slides). **a** Class I, small fibrotic area in the centre of the tumour, less than 25 % of the microscopic

field. **b** Class II, dense fibrous stroma occupies about half of the tumour (between 25 and 50 %). **c** Class III, tumour with prevalent sclerotic tissue (more than 50 % of the histological field)

Table 1 Results: pathologic characteristics of lesions

MDCT pattern	Histological type		
	Wdt-b	Wdt-u	WDC
A (adCT 11 mm)	12 (adH 9 mm)	7 (adH 14 mm)	0
B1 (adCT 31 mm)	7 (adH 11 mm)	8 (adH 21 mm)	14 (adH 40 mm)
B2 (adCT 44 mm)	0	0	12 (adH 42 mm)

Wdt-b well-differentiated tumour–benign behaviour, *Wdt-u* well-differentiated tumour–uncertain behaviour, *WDC* well-differentiated carcinoma

and reconstruction was carried out in 4 patients. Liver metastases were resected in 9 patients and sampled in the remaining 2. Lymphadenectomy was carried out in 40 patients.

Pathology of pNETs and correlation with MDCT pattern

Tables 1 and 2 summarize the histological characteristics of the 60 lesions.

All 60 tumours were confirmed to be pNETs. According to the 2004 WHO classification system all tumours were classified as well-differentiated tumours (Wdt), 19 (32 %) of which with benign behaviour (Wdt-b), 15 (25 %) with uncertain behaviour (Wdt-u) and 26 (43 %) as well-differentiated carcinomas (WDC).

At pathology (Table 1) 12 out of 19 (63 %) A lesions were classified as Wdt-b [5–15 mm; average diameter at histology (adH) 9 mm]. The remaining 7 pNETs with type A CEP were all classified as Wdt-u (8–22 mm; adH 14 mm). Interestingly, no pNET with type A CEP was a WDC. Fourteen out of 29

Table 2 Characteristics of lesions

Histological data	MDCT pattern		
	A	B1	B2
WHO grade			
Wdt-b	12	7	0
Wdt-u	7	8	0
WDC	0	14	12
ENETS			
G1	17	21	2
G2	2	7	10
G3	0	1	0
Dimension			
<2 cm	17	10	1
≥2 cm	2	19	11
Angioinvasion			
Present	2	16	12
Absent	17	13	0

Wdt-b well-differentiated tumour–benign behaviour, *Wdt-u* well-differentiated tumour–uncertain behaviour, *WDC* well-differentiated carcinoma

(48 %) B1 lesions were WDC (14–70 mm; adH 40 mm), 8 Wdt-u (7–50 mm; adH 21 mm) and 7 Wdt-b (5–20 mm; adH 11 mm). Note that all 12 pNETs showing type B2 CEP were WDC (12–67 mm; adH 42 mm). Overall, type A CEP was associated with a positive predictive value (PPV) of 63 % when assessing for Wdt-b, while type B CEP was associated with a negative predictive value (NPV) of 83 % when assessing for Wdt-b and a PPV of 63 % when assessing for WDC.

Considering lesion size, 11 lesions less than 2 cm but showing type B CEP were classified as Wdt-u (9 tumours) or WDC (2 lesions); 4 out of 34 (12 %) lesions of at least 2 cm were WDC.

Sensitivity and specificity in detection of non-benign lesions were 83 % and 63 % according to CEP and 76 % and 95 % according to lesion dimension; by combining both CEP and size, sensitivity and specificity increased up to 95 % and 73 % respectively.

Type of CEP was indeed strongly related to tumour histology ($p < 0.0001$) and tumour diameter ($p < 0.0001$) (Fig. 5). Concerning the latter, in particular, an excellent correlation ($R = 0.9$) was noted between MDCT and histology. Size concordance was even more evident ($R = 0.91$) when pNETs becoming hyperdense in the early phases of MDCT (type A and B1 CEP) were considered together, and decreased ($R = 0.85$), despite remaining high, in pNETs showing type B2 CEP.

Ki67 values ranged between 0.5 and 30 %, being at most 2 % (G1 according to the ENETS grading system) in 40 cases, between 3 and 20 % (G2) in 19 cases and greater than 20 % (G3) in 1 case. Significant differences ($p < 0.0001$) between A and B lesions were found (Fig. 6): Ki67 values of A lesions ranged between 0.5 % and 3 %, being 17/19 (89 %) lesions classified as G1 and 2 as G2; Ki67 values of B lesions ranged between 0.5 % and 30 % (23/41 G1, 17/41 G2 and 1 G3). In particular, 21 out of 29 (72 %) B1 lesions were classified as G1, 7 as G2 and 1 as G3 (with Ki67 values ranging

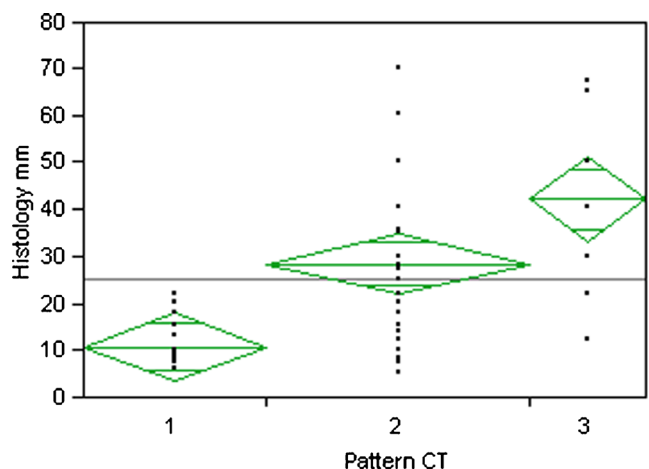


Fig. 5 Scatter plot depicting the histological diameter of lesions, grouped by CEP. The black lines represent the average diameter at histology (adH)

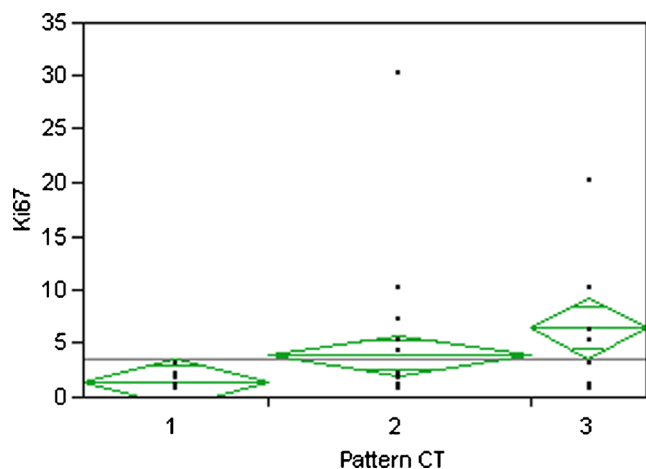


Fig. 6 Scatter plot representing the distribution of Ki67 values among the three CEP

between 0.5 % and 30 %); Ki67 values of B2 lesions ranged between 0.5 % and 20 %, with 10/12 (83 %) classified as G2 and 2 as G1.

Angioinvasion was present in all 12 patients with B2 lesions, in 15/26 (58 %) patients with B1 lesion and in 2/13 (15 %) patients with A lesions alone, with significant difference ($p < 0.0001$) between A and B lesions.

Vascular venous infiltration was confirmed in 3 out of 4 resected veins, nodal metastases in 17 out of 40 patients submitted to lymphadenectomy and liver metastases in all 11 cases submitted to hepatic resection or sampling. Table 3 summarizes the characteristics of the patients. Lymph node metastases were present only in patients with B lesions ($p < 0.0001$) and, in particular, they were demonstrated in 10/

12 patients with B2 lesions (83 %) and 7/29 patients with B1 lesions (27 %); hepatic metastases were present in 8 patients with B2 lesions (67 %) and 2 B1 lesions (8 %).

The distribution of patients among the different stages (AJCC–UICC and ENETS respectively) demonstrated a significant correlation ($p < 0.0001$) between the CEP and stages, considering both systems of staging.

Correlation between MDCT pattern and MVD

Table 4 summarizes the distribution of MVD average values among patterns and histological subtypes. The MVD values ranged between 497 and 65 vessels/mm². The MVD values ranged between 497 and 214 vessels/mm² in WDt-b, between 387 and 135 vessels/mm² in WDt-u and between 415 and 65 vessels/mm² in WDC. The MVD values ranged between 497 and 279 vessels/mm² in A lesions, between 481 and 87 vessels/mm² in B1 lesions and between 280 and 65 vessels/mm² in B2 lesions (Fig. 7). Differences among the three groups were statistically significant, both by considering the three different histological types ($p < 0.0001$) and the three different patterns ($p < 0.0001$).

Fibrosis

The comparative examination of A, B1 and B2 lesions revealed the absence of fibrosis in all A lesions, while its presence was detected in 24/29 (83 %) B1 lesions and 10/12 (83 %) B2 lesions. In particular in B1 lesions fibrosis was rated as class I, class II and class III in 10, 8 and 6 cases respectively; in 8/10 B2 lesions fibrosis was graded as class II, while only 1 case was found in classes I and III (Table 5).

For the 5 cases of B1 and B2 lesions without fibrosis, we searched for another histological characteristic that could explain their delayed enhancement and found that they all featured spaces with blood stagnation. Such a histological finding was not seen in any of the A lesions.

Table 3 Characteristics of patients

Histological data	MDCT pattern		
	A	B1	B2
Lymph node metastases			
Present	0	7	10
Absent	14	19	2
AJCC–UICC			
Ia	12	11	0
Ib	2	6	1
IIa	0	1	0
IIb	0	6	2
III	0	0	0
IV	0	2	9
ENETS			
I	13	9	0
II	1	8	1
IIIa	0	1	0
IIIb	0	6	2
IV	0	2	9

Table 4 Results: MVD of lesions *WDt-b* well-differentiated tumour–benign behaviour, *WDt-u* well-differentiated tumour–uncertain behaviour, *WDC* well-differentiated carcinoma

MDCT pattern	Histological type		
	WDt-b (379±90)	WDt-u (296±90)	WDC (189±91)
A (386±71)	12 (401±84)	7 (358±31)	0
B1 (249±107)	7 (340.7±92.3)	8 (243±82)	14 (207±101)
B2 (168±77)	0	0	12 (168±77)

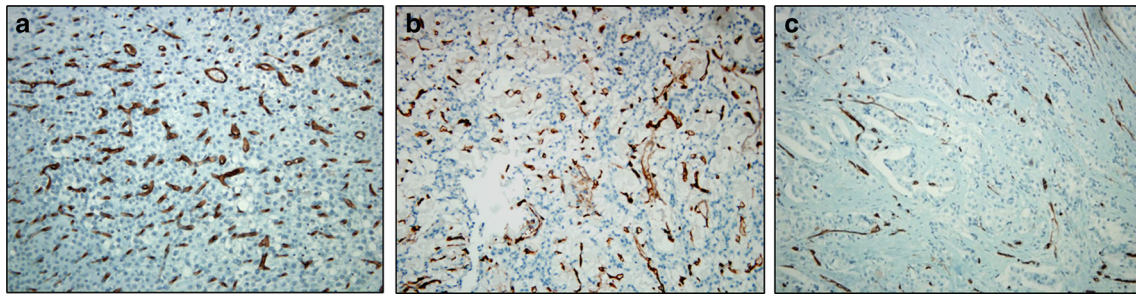


Fig. 7 MVD (CD34 monoclonal antibody staining): **a** Tumour with high number of vessels in pattern A. **b** Tumour with intermediate grade of vascularity in pattern B1. **c** Low number of vessels in pattern B2 tumour. (Original magnification $\times 20$)

Discussion

In the evaluation of pNETs, imaging plays a pivotal role for suggesting the best therapeutic approach, allowing the localization of functioning neoplasms, the differential diagnosis with respect to other pancreatic tumours or non-tumoral pancreatic masses [21], the identification of signs of malignancy and the local and distant staging [21–23]. The novel finding provided by our study is represented by the fact that CEP of pNETs, as defined during a standardized multiphasic MDCT study, even if conducted by using scanners of different generations, provides information matching all histological parameters of prognostic relevance and could therefore be used to predict the course of pNETs. As compared with previous methods [19, 24–26] in which images were acquired only in the early arterial, pancreatic and venous phases, we decided to add a scan in the late phase, 3 min after contrast injection, because some pNETs show progressive enhancement, becoming more conspicuous in this phase. pNETs are expected to be hypervascular [6, 27] because of their origin from the highly vascularized islet cells, which receive 10–20 % of the entire pancreatic supply, thanks to the presence of windowed capillaries, whose morphology and distribution ensure a rapid capillary exchange in normal conditions. A near-normal architecture and function of tumour capillaries is expected to be maintained in benign tumours despite the strong angiogenic impulse in pNETs [28]. On the contrary, progression towards malignancy is associated with derangement in vessel architecture and function. Despite these tumours remaining hypervascular, their anarchic vasculature is reflected by their less homogenous CEP; in particular delayed contrast

enhancement may be considered as a sign of malignancy in pNETs [27, 29–32]. In fact, previous studies reporting on pNET characteristics at MDCT have demonstrated that benign tumours are usually small, showing a homogenous hypervascular pattern after contrast injection followed by early wash-out in the venous phase. On the contrary, larger pNETs have a less homogeneous CEP and are associated with greater malignant potential, especially in the presence of necrosis and calcifications [19–22]. From a practical point of view, however, when obvious markers of malignancy are lacking, preoperative anticipation of tumour grade in pNETs is based on tumour size.

In our study, CEP was statistically related to tumour histology ($p < 0.0001$); in particular, while no pNET showing type A CEP eventually proved to be malignant, all pNETs showing type B2 CEP corresponded to WDC. On the other hand, results of the present study underline that B1 pNETs remain ‘uncertain’ lesions, whose aggressiveness cannot be affirmed on the basis of the CEP alone, while they can be further differentiated according to their dimension (see Table 1). The correlation between CEP and tumour biology was so evident that 11 small pNETs measuring less than 2 cm but showing type B CEP were eventually classified as WDt-u (9 tumours) or WDC (2 lesions); moreover 4/34 (12 %) lesions measuring at most 2 cm were WDC. Sensitivity in detection of non-benign lesions was higher according to CEP than according to lesion size (83 % and 76 % respectively).

Furthermore, comparison between pNET size at MDCT and at histology showed a good correlation between MDCT and histology for B2 lesions, and an excellent correlation for tumours having early contrast enhancement (type A and type B1 CEP). The latter correlation, in particular, may be justified by an improved delineation of tumour boundaries thanks to the strong and more homogeneous enhancement of these lesions. On the other hand, this observation underscores that size measurement may be less reliable in pNETs showing type B2 CEP, which, unfortunately, is the category at higher risk of malignant histology. This issue, of course, is not relevant for large pNETs, for which therapeutic decisions follow straightforwardly, but rather for tumours around 2 cm in diameter for which the exact definition of tumour size is crucial for

Table 5 Results: fibrosis evaluation

MDCT pattern	Fibrosis		
	Class I	Class II	Class III
A	0	0	0
B1	10	8	6
B2	1	8	1

therapeutic counselling. Note that in this series there were 8 WDC with the greatest diameter around 2 cm, of which 4 showed type B2 CEP.

In these series CEP showed a significant correlation with other all conventional post-surgical prognostic indicators (including tumour stage, either AJCC–UICC or ENETS, angioinvasion, presence of lymph node metastases and Ki67 percentage) that, however, cannot be fully assessed until the tumour is resected and thoroughly examined. Angioinvasion was demonstrated in all patients with pNETs showing type B2 CEP but only in two patients with type A pNETs ($p < 0.0001$). Lymphatic metastases were demonstrated only for patients with type B pNETs, and were highly prevalent in tumours with type B2 CEP (83 %). Interestingly, CEP of pNETs demonstrated significant correlation with the ENETS tumour grading, whose prognostic value has been established [3, 14–17]: nearly all (89 %) type A pNETs Ki67 values led to grade G1, while 83 % of type B2 pNETs were graded as G2.

Moreover, our findings on MVD support those of previous reports [33, 34] demonstrating that, conversely to what happens with other neoplasms, pNETs present an inverse relation between the MVD and the differentiation grade (the MVD being significantly lower in carcinomas). In fact, Rodallec et al., following a dual-phase helical CT protocol, have already shown a correlation between tumour MVD and the enhancement during the pancreatic phase, as poorly differentiated carcinomas were less vascularized than WDt and WDC [35]. In this study, poor contrast enhancement during the pancreatic phase also portended shorter patient survival because of the association with higher tumour grade. However, no distinction was made among differentiated pNETs (i.e. WDt-b, WDt-u and WDC) on the basis of their CEP, which are instead pNETs posing the greatest challenges in therapeutic counselling.

In a more recent study on CT perfusion, D'Assignies and coll. confirmed that tumour vascularization is strongly related to MVD on tumour histology ($p < 0.0001$) and that some perfusion parameters predict tumour type and prognosis after treatment [33]. However, perfusion CT examination confers an additional radiation dose, requiring dedicated, additional examination after the tumour has been already identified at a previous CT. Thus, perfusion CT is clearly neither the standard nor a practical examination to use in the preoperative evaluation of pNETs.

Results of our study demonstrated significant differences in MVD values among the 3 CEP, with B2 cases showing the lowest values of MVD, confirming that meticulous definition of CEP of pNETs could provide a surrogate marker of malignancy and support therapeutic planning, especially in the case of small asymptomatic tumours.

However, the difference in the MVD between the A and B pattern may justify the difference in the degree of enhancement, while it does not justify the different timing of the

enhancement. Hence, in addition, we compared A and B lesions by analysing other histological findings that could explain such different behaviour. In fact, B2 lesions show findings typical of a more aged disease, including macrophages filled with haemosiderin pigment and fibrosis; the latter can justify the late enhancement of these lesions, such as in other tumours with similar desmoplastic component. In lesions presenting a B CEP without fibrosis the delayed enhancement was justified by the presence of abnormally dilated cystic spaces, with blood stagnation and thrombosis, as previously reported in some studies [30–32].

Therefore, MVD and other histological findings (fibrosis in particular) determine the different CEP of pNETs, in terms of degree and timing of enhancement. B1 lesions, maintaining the hypervascularization of A lesions (characterized by high MVD) and presenting lower amounts of fibrosis than B2 lesions, show an intermediate behaviour, with early enhancement, persistent in late phases.

One possible limitation of this study could be the lack of poorly differentiated carcinomas, as defined by the 2004 WHO classification, within our study population. This could be explained by the fact that our correlation between MDCT parameters and histology findings required tumour resection, whereas patients with poorly differentiated endocrine carcinomas are generally not referred for surgery. On the other hand, poorly differentiated pNET are often associated with obvious radiologic markers of malignancy, making CEP often unnecessary to anticipate tumour grade. However the inclusion of all well-differentiated lesions can further validate our results, allowing the use of CEP to suggest the pNET behaviour in the early steps of tumour dedifferentiation.

In conclusion, CEP of pNETs, as determined during multiphase MDCT study, correlates with their histological grading and other prognostic predictors, allowing one to predict their biological behaviour. On the basis of the present results, a lesion showing type A CEP can be reasonably considered as benign; on the contrary, type B2 CEP should be considered strongly suggestive of malignancy. Therefore, CEP can provide reliable information that could be used to support decisions on pNETs treatment. Such information could have relevance in deciding the extent of resection or in deciding not to refer the patient to surgery and implement a policy of follow-up. With respect to the latter, which is more often reserved to small asymptomatic pNETs, our data indicate that a conservative approach should be considered with greater concern in tumours showing type B2 CEP.

Acknowledgments The scientific guarantor of this publication is Salvatore Mazzeo M.D. The authors of this manuscript declare no relationships with any companies whose products or services may be related to the subject matter of the article. The authors state that this work has not received any funding. No complex statistical methods were necessary for this paper. Institutional review board approval was not required because our study is a retrospective review of standard preoperative CT

examinations. Written informed consent was not required for this study because our study is a retrospective review of standard preoperative CT examinations. Methodology: retrospective, diagnostic or prognostic study, performed at one institution.

Conflict of interest None.

References

- Asa SL (2011) Pancreatic endocrine tumors. *Mod Pathol* 24(Suppl 2):S66–S77
- Klöpffel G, Rindi G (2010) The ENETS and AJCC/UICC TNM classifications of the neuroendocrine tumors of the gastrointestinal tract and the pancreas: a statement. *Virchows Arch* 456:595–597
- Klöpffel G (2011) Classification and pathology of gastroenteropancreatic neuroendocrine neoplasms. *Endocr Relat Cancer* 18(Suppl 1):S1–S16
- Klimstra DS, Modlin IR (2010) The pathologic classification of neuroendocrine tumors; review of nomenclature, grading, and staging systems. *Pancreas* 39:707–712
- De Lellis RA, Lloyd RV (2004) Pathology and genetics of tumors of endocrine organs. IARC, Lyons
- Klöpffel G, Rindi G (2007) Site-specific biology and pathology of gastroenteropancreatic neuroendocrine tumors. *Virchows Arch* 451(Suppl 1):S9–S27
- Rindi G (2010) The ENETS guidelines: the new TNM classification system. *Tumori* 96:806–809
- Rindi G, Wiedenmann B (2012) Neuroendocrine neoplasms of the gut and pancreas: new insights. *Nat Rev Endocrinol* 8:54–64
- Edge SB, Byrd DR (2009) AJCC cancer staging manual, 7th edn. Springer, New York
- Scarpa A, Mantovani W (2010) Pancreatic endocrine tumors: improved TNM staging and histopathological grading permit a clinically efficient prognostic stratification of patients. *Mod Pathol* 23:824–833
- Hamilton NA, Liu TC (2012) Ki-67 predicts disease recurrence and poor prognosis in pancreatic neuroendocrine neoplasms. *Surgery* 152:107–113
- Anlauf M (2011) Neuroendocrine neoplasms of the gastroenteropancreatic system: pathology and classification. *Horm Metab Res* 43:825–831
- Schmitt AM, Anlauf M (2007) WHO 2004 criteria and CK19 are reliable prognostic markers in pancreatic endocrine tumors. *Am J Surg Pathol* 31:1677–1682
- Ekebald S, Skogseid B (2008) Prognostic factors and survival in 324 patients with pancreatic endocrine tumor treated at a single institution. *Clin Cancer Res* 14:7798–7803
- Fisher L, Kleeff J (2008) Clinical outcome and long term survival in 118 consecutive patients with neuroendocrine tumors of the pancreas. *Br J Surg* 95:627–635
- La Rosa S, Klersy C (2009) Improved histologic and clinicopathologic criteria for prognostic evaluation of pancreatic endocrine tumors. *Hum Pathol* 40:30–40
- Scarpa A, Mantovani W (2010) Pancreatic endocrine tumors: improved TNM staging and histopathological grading permit a clinically efficient prognostic stratification of the patients. *Mod Pathol* 23:824–833
- Rodallec M, Vilgrain V (2006) Endocrine pancreatic tumours and helical CT: contrast enhancement is correlated with microvascular density, histoprognostic factors and survival. *Pancreatology* 6:77–85
- Couvelard A, O’Toole D (2005) Microvascular density and hypoxia-inducible factor pathway in pancreatic endocrine tumours: negative correlation of microvascular density and VEGF expression with tumour progression. *Br J Cancer* 92:94–101
- D’Assignies G, Couvelard A (2009) Pancreatic endocrine tumors: tumor blood flow assessed with perfusion CT reflects angiogenesis and correlates with prognostic factors. *Radiology* 50:407–416
- Horton KM, Hruban RH (2006) Multi-detector row CT of pancreatic islet cell tumors. *Radiographics* 26:453–464
- Pereira PL, Wiskirchen J (2003) Morphological and functional investigations of neuroendocrine tumors of the pancreas. *Eur Radiol* 13:2133–2146
- Kulke MH, Anthony LB (2010) North American Neuroendocrine Tumor Society (NANETS). NANETS treatment guidelines: well-differentiated neuroendocrine tumors of the stomach and pancreas. *Pancreas* 39(6):735–752
- Marion-Audibert AM, Barel C (2003) Low microvessel density is an unfavorable histoprognostic factor in pancreatic endocrine tumors. *Gastroenterology* 125:1094–1101
- Takahashi Y, Akishima-Fukasawa Y (2007) Prognostic value of tumor architecture, tumor-associated vascular characteristics, and expression of angiogenic molecules in pancreatic endocrine tumors. *Clin Cancer Res* 13:187–196
- Jani N, Moser AJ (2007) Pancreatic endocrine tumors. *Gastroenterol Clin N Am* 36:431–439
- Oberg K, Eriksson B (2005) Endocrine tumours of the pancreas. *Best Pract Res Clin Gastroenterol* 19:753–781
- Rockall AG, Reznick RH (2007) Imaging of neuroendocrine tumours (CT/MR/US). *Best Pract Res Clin Endocrinol Metab* 21:43–68
- Bergers G, Benjamin LE (2003) Tumorigenesis and the angiogenic switch. *Nat Rev Cancer* 3:401–410
- Fidler JL, Johnson CD (2001) Imaging of neuroendocrine tumors of the pancreas. *Int J Gastrointest Cancer* 30:73–85
- Koito K, Namieno T (1997) Delayed enhancement of islet cell carcinoma on dynamic computer tomography: a sign of its malignancy. *Abdom Imaging* 22(3):304–306
- Ichikawa T, Peterson MS (2000) Islet cell tumor of the pancreas: biphasic CT versus MR imaging in tumor detection. *Radiology* 216:163–171
- Anlauf M, Sipos B (2005) Tumors of the endocrine pancreas. *Pathologe* 26:46–51
- Thoeni RF, Mueller-Lisse UG (2000) Detection of small, functional islet cell tumors in the pancreas: selection of MR imaging sequences for optimal sensitivity. *Radiology* 214:483–494
- Moayedoddin B, Booya F (2006) Spectrum of malignant somatostatin-producing neuroendocrine tumors. *Endocr Pract* 12:394–400